iScience

CellPress
OPEN ACCESS

Article

Integrated physiological analyses, transcriptome, and DNA methylation reveal superiority of pear stigma-style complex development regulation

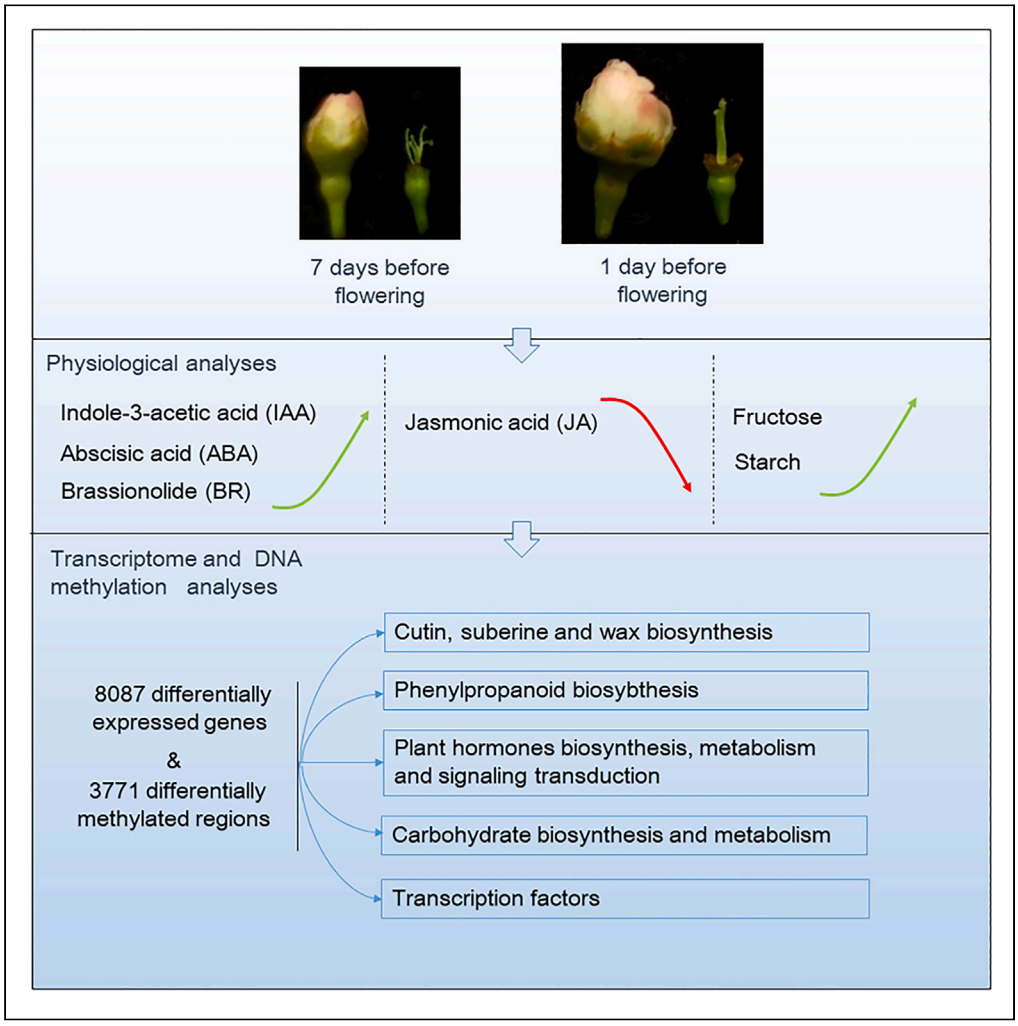

Xu Huang, Li-Hua Zhai, Xiao-Xiong Kong, Jing Zhang, Xiao Liu, Chun-Lei Wang

wangcl@yzu.edu.cn

Highlights

IAA, ABA, and BR increased during pear stigma-style complex development

ERFs are involved in regulating the development of fruit plant style and stigma

Most DMRs of CHH were upregulated during pear stigma-style complex the development

Huang et al., iScience 27, 110372
July 19, 2024
https://doi.org/10.1016/j.isci.2024.110372

iScience

CellPress
OPEN ACCESS

Article

Integrated physiological analyses, transcriptome, and DNA methylation reveal superiority of pear stigma-style complex development regulation

Xu Huang,[1] Li-Hua Zhai,[1] Xiao-Xiong Kong,[1] Jing Zhang,[1] Xiao Liu,[1] and Chun-Lei Wang[1,2,*]

SUMMARY

Styles and stigmas are crucial components of the fertilization process that allows a pear tree to bear fruit. The information regarding the development mechanism of pear style and stigma is still unclear. Our results demonstrated that IAA, ABA, and BR are significantly increased at 1 DBF, while JA is decreased at 5 DBF. The fructose and starch contents significantly increased at 1 DBF when the style with stigma was ready for pollination. Transcriptome and DNA methylation analysis showed 8087 DEGs and 3771 DMRs were enriched in plant hormones biosynthesis, carbohydrate biosynthesis and metabolism, and TFs in 1 DBF as compared with 7 DBF. The CHH methylation type of DMRs accounts for 84.75%. Most DMRs of CHH upregulated in 1 DBF vs. 7 DBF. This study found for the first time that transcription factor ERFs and DNA methylation are involved in regulating the growth and development of fruit plant style and stigma.

INTRODUCTION

In angiosperms, the gynoecium forms the female reproductive organ and develops into fruit after fertilization.[1] The pistil is a complex tissue structure established through a polar system. It is a model to study the tissue differentiation of multicellular organisms. Style and stigma are important components of the pistil that plays a crucial role in identifying pollen species, promoting pollen germination, guiding pollen tubes to ovule growth, and completing fertilization.[2] Moreover, appropriate style length plays an important role in guiding pollen tube growth and ensuring the completion of pollination and fertilization.[2]

Based on the transmitting function and anatomy, style can be divided into three types: open, closed, or semi-closed.[3] The open style is usually present in monocots, has a canal lined with a glandular epidermis or epithelium; the closed style is characterized by a core of transmitting tissue and is more common among the eudicots; and the semi-closed style has a canal limited by the transmitting tissue. It is considered that style development is the result of the cross-talk of plant hormones. Auxin signaling plays a central role in style elongation. Recently, leaf polarity regulators have been reported to affect style length through auxin dynamics in *Mimulus lewisii* plant.[4] It is found that the *Nicotiana* genus-specific jasmonic acid (JA)-deficient short-style phenotype was induced by alterations in 17-hydroxygeranyllinalool diterpene glycosides (DTGs) malonylation patterns. DTG-dependent reduced floral style lengths resulted from reduced stylar cell sizes, IAA contents, and YUC activity.[5,6] In addition, gibberellin (GA) and brassinosteroid (BR) also affect the style cell elongation. *SYL3-k* allele increases style length by enhancement of endogenous content GA_4 in *Oryza sativa* L..[7] In *Primula*, *CYP734A50* gene, encoding a putative BR-degrading enzyme, is only present on the short-styled S-morph haplotype, its loss or inactivation leads to long styles, and exogenous BR treatment could convert the short style to a long style.[8] At the same time, gene expression at certain developmental stages is also important for style development, significant differences in the expression of auxin and BR synthesis-related genes between male and female flowers at different developmental stages were detected in papaya.[9] Recently, it has been discovered that epigenetics are also involved in the regulation of style development. It is found that Lch-lnc7374-miR156j-*SPL9* were potential regulators of pistil development in *Liriodendron chinense*.[10] And, mutation in *OsRDR2* decreased genome-wide CHH methylation, and disturbed male and female reproductive development in rice.[11] There is no report on whether epigenetics are involved in the development of fruit tree styles.

The stigma is the receptive portions of the pistil, which is covered by a modified epidermis. In relation to its modified epidermis surface dry or wet, stigmas can be classified into two different type: dry, or wet.[12] The dry stigma is constituted by a papillary primary cell wall, a waxy cuticle and a proteinaceous pellicle.[13] In wet stigmas, a notable amount of viscous fluid is excluded by papillae and the subtending stigmatic cells. The viscous fluid contains polysaccharide, pigments, and many kinds of proteins.[13,14] When pollen falls onto the stigma, the proteins on the surface of the pollen and the stigma recognize each other, thereby determining the fate of the pollen. The development of the stigma often develops together with other floral organ.

[1]College of Horticulture and Landscape Architecture, International Research Laboratory of Agriculture and Agri-Product Safety, Key Laboratory of Plant Functional Genomics of the Ministry of Education, Yangzhou University, 48 Wenhui East Road, Yangzhou 225009, People's Republic of China
[2]Lead contact
*Correspondence: wangcl@yzu.edu.cn
https://doi.org/10.1016/j.isci.2024.110372

Pear is ranked in the top five fruit sales globally, therefore fruit production is critical to the industry and this requires a well-developed gynoecium and good pollination. In *Pyrus* spp., the pistil is composed of 2–5 carpels with fused ovaries. The Asiatic pears usually have 5-loculed ovary with the same number of glabrous styles with punctate stigmas. Pear has a closed style and wet stigma. Both style and stigma secreted an extracellular fluid necessary for the pollen grain germination and pollen tube growth.[15] As a self-incompatible fruit tree, both compatible and incompatible pollen can hydrate and then germinate into the stigma after falling on the stigma. The incompatible pollen tubes stopped growing due to the action of a self-incompatible factor, S-RNase, in style.[16] So far, the ultrastructure of stigmatic and stylar has been studied.[15,17] There is a large amount of transmitting tissue that is surround by parenchymatous cells with vascular bundles and rimmed by epidermis in style. There are numerous endoplasmic reticulum present at both the stigma and stylar transmitting tissue.[15] So far, the genes involved in the regulation of style and stigma development are even less clear. The genetic changes during the development of pistils have only been studied in a few fruit trees such as papaya and apricot.[9,18,19] However, there have been no reports on the involvement of DNA methylation in the development of fruit tree styles. Therefore, studying the genetic changes and DNA methylation levels during the development of styles and stigma of pear is of great significance for revealing the regulatory mechanisms of style and stigma development.

RESULTS

State of length, hormone and carbohydrate contents during pear styles growth

To obtain the characterization of pear styles during the development process, the styles of flower 7 days (7 DBF), 5 days (5 DBF), 3 days (3 DBF), 1 day (1 DBF), or 0 days (0 DBF) before flowering were collected (Figure 1A). The length of the style was measured first. We found the length of styles increased most rapidly from 7 DBF to 3 DBF; the growth rate of the styles was about 0.83 mm per day (Figure 1B). And from 3 DBF to 1 DBF, the growth rate of the styles decreased a little, about 0.56 mm per day (Figure 1B). Finally, the length of styles no longer increased from 1 DBF to 0 DBF (Figure 1B). At the same time, we measured the contents of indole-3-acetic acid (IAA), abscisic acid (ABA), brassinolide (BR), and jasmonic acid (JA) of the pear styles (Figures 1C–1F), which have been reported to be related to style growth.[5,8,18] The study found that IAA, ABA, BR had a significant increase from 3 DBF d to 1 DBF (Figures 1C, 1E, and 1F), and JA had a significant decrease from 7 DBF to 5 DBF (Figure 1D). Considering that the rapid growth of styles occurs from 7 DBF to 3 DBF, which indicate these hormones have little relationship with the rapid growth of style.

In addition, the pear style is a wet style and these secretions contain polysaccharide, pigments, and many kinds of proteins, which promote pollen germination and pollen tube growth. In order to understand sugars changes during style development, the contents of sucrose, glucose, fructose and starch were analyzed at the five-style development time (Figures 1G–1J). The sucrose content decreased at 3 DBF and maintained stability during other periods (Figure 1G); the highest glucose content showed at 7 DBF, then the content decreased and remained stable (Figure 1H). But there was no significant differences observed from 5 DBF to 1 DBF in glucose content (Figure 1H). The content of sucrose or glucose increased at 1 DBF when the style was ready for pollination. The changing trend of fructose and starch content is the same as that of BR, IAA, and ABA (Figures 1I and 1J). The fructose content was increased at 1 DBF (Figure 1I), and the starch content in the style showed increased, decreased, and then increased again (Figure 1J).

Transcriptome analysis of styles during growth

We performed a comparative RNA sequencing analysis to gain further insight into the molecular mechanism modulating style growth. As the pear styles were observed to have continuous growth from 7 days (7 DBF) to 1 day (1 DBF) before flowering, the style at 7 DBF and 1 DBF were selected for cDNA library construction. Approximately 6.5 Gb data on average were generated form each sample. Also, 129,920,568 and 131,780,526 clean reads with a Q30 percentage of 93% were obtained from the 1 DBF styles and 7 DBF styles sample, respectively (Table S2). In total, 80.71% of clean reads from the 7 DBF styles and 81.55% from the 1 DBF styles were mapped to the reference genome. These results indicated that the sequencing data were sufficient for further high-accuracy functional annotation.

The correlation coefficient of gene expression levels between biological replicates for all samples was greater than 0.952 (Figure 2A), indicating that the biological replicates were suitable for DEG screening. Based on a standard estimated absolute $\log_2$(fold change) $\geq$ 1 and correlated *p*-value $\leq$0.05, 2993 genes that were upregulated and 5094 genes that were downregulated were identified in the 1 DBF styles sample compared to the 7 DBF (Figure 2B; Table S3). To identify genes linked to the trait of interest, the selected DEGs were functionally annotated according to the content within the GO database. Of the 8087 DEGs, 7741 were divided into biological process (36.94%), cellular component (10.94%) and molecular function (52.11%) (Figure 2C).

Moreover, the DEGs were also mapped to the KEGG pathway database. KEGG pathway enrichment analysis showed that the DEGs were most significantly enriched in the biosynthesis of other secondary metabolites (299 members), metabolic pathways (228 members), plant hormone signal transduction (106 members), and plant-pathogen interaction (91 members). Biosynthesis of other secondary metabolites mainly contains starch and sucrose metabolism (77 members) and phenylpropanoid biosynthesis (73 members). Additionally, some pathways related to the biosynthesis of plant hormones (total 119 members), such as alpha-Linolenic acid metabolism, Carotenoid biosynthesis, tryptophan metabolism and brassinosteroid biosynthesis (Figure 2D).

DNA methylation analysis of style during style growth

Using whole-genome bisulfite sequencing (WGBS) technology, each sample yielded about 14 Gb of clean bases, the average alignment rate of each sample reached 64.5%, Clean reads with a Q30 percentage is from 89.76% to 90.2%, indicating that the methods used in our study were

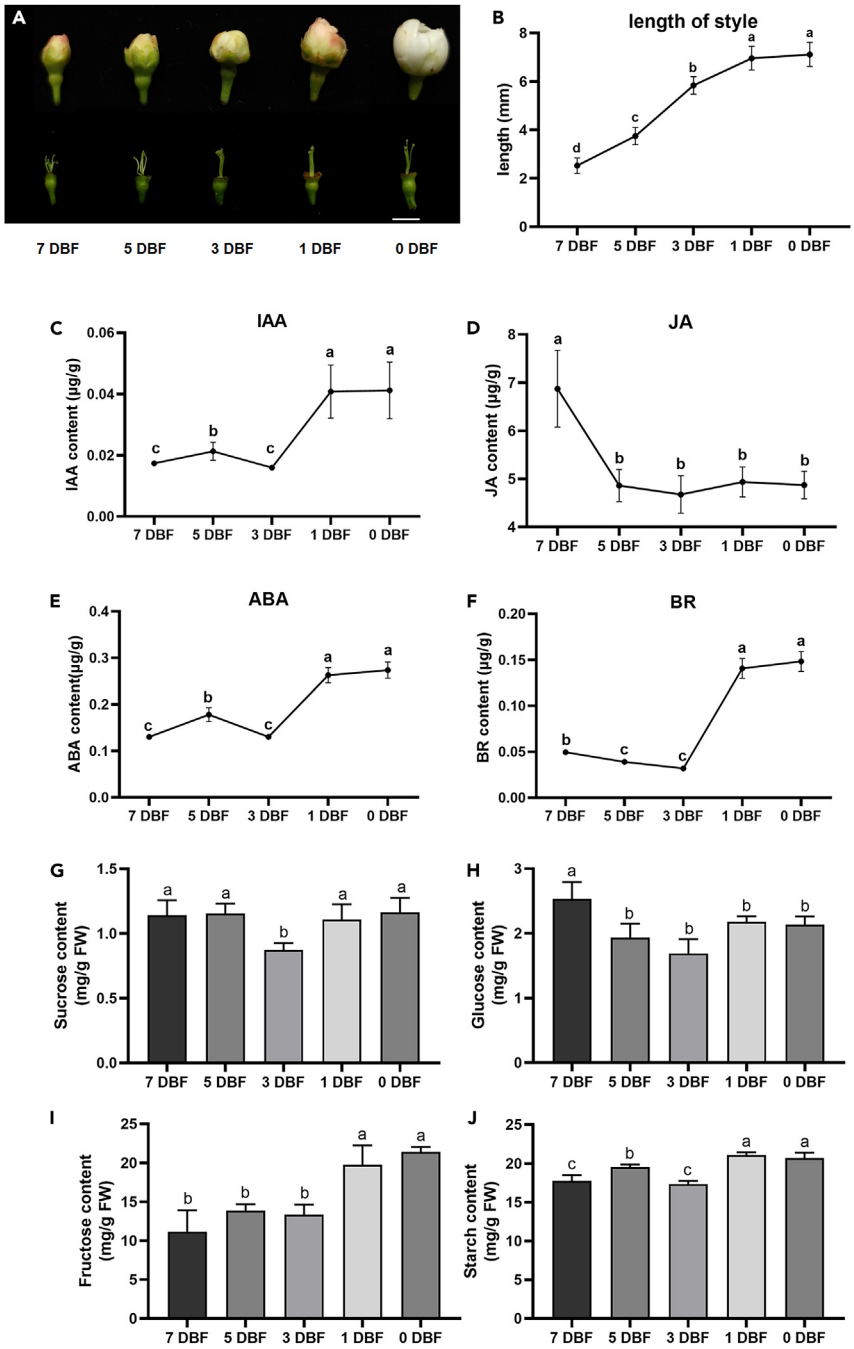

Figure 1. Physiological analyses during styles growth

(A–B) The image (A) and length of pear styles (B) in each growth period. Bar = 1 cm. (C–F) IAA (C), JA (D), ABA (E), BR (F) changes of pear styles in each growth period. (G–J) Sucrose (J), glucose (H), fructose (I) and starch (J) contents of pear styles in each growth period. DBF means day before flowing. Values are presented as means ± SE with three biological replicates. Different letters above bars indicate significant differences between values ($p < 0.05$). Same letters above bars indicate no significant differences between values.

reliable and the results accurate (Table S4). Circos plots were used to exhibit differences in genome-wide methylation levels in 1 DBF compared to the 7 DBF. The differentially methylated regions (DMRs) were distributed across all 17 chromosomes in the two-style sample (Figure 3A). Furthermore, 3771 DMRs were identified in 1 DBF compared to the 7 DBF (Table S5). Among these DMRs, mCHH (3196, 84.75%) accounted for the highest percentages (Figure 3B). More than two-thirds of DMRs are located in the promoter region (Figure 3C). Compared to the 7 DBF, DMRs of CHH show increase in methylation rate at 1 DBF. However, DMRs of CG and CHG show decrease in methylation rate (Figures 3D–3F).

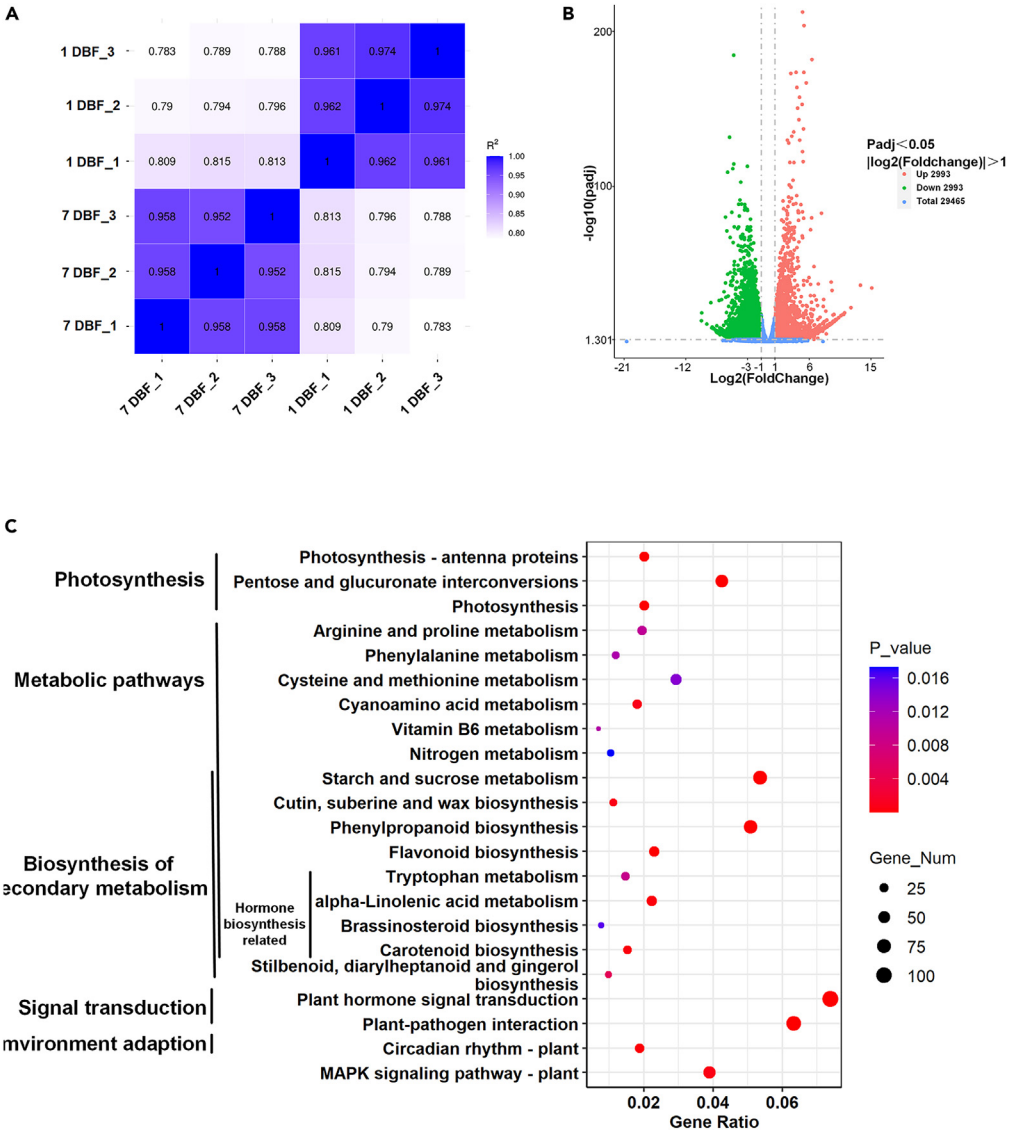

Figure 2. Identification and expression analysis of the differentially expressed genes (DEGs) involved style growth regulation

(A) Correlation analysis between the 1 DBF and 7 DBF styles samples with three biological replicates.

(B) Volcano plot filtering identified genes differentially expressed in the 1 DBF and 7 DBF styles groups.

(C) Scatterplot of the DEGs identified significantly enriched KEGG pathways.

The distribution of the DNA methylation of different transcription elements was similar in high methylation rates occurring in promoter and intron regions (Figures 3E–3I). As shown in Figures 3J–3L, regarding the number of DMRs, the CHH type is the most, followed by the CG type, and the CHG type is the least. CHH-type DMRs are mainly hyper. But CG and CHG-type DMRs are the opposite, most are hypo.

KEGG enrichment analyses were performed to better understand the function of DMRs in style growth. We selected mainly genes with DMRs in the 2 kb upstream promoter region for the enrichment analysis. With the standard of p-value ≤ 0.05, DMRs were significantly enrich in 'metabolic pathways' (196 members) and 'biosynthesis of secondary metabolites' (104 members), 'Plant hormone signal transduction' (25 members) (Figure 4).

Consistency and linear regression analysis between qRT-PCR and RNA-seq, qRT-PCR and WGBS

To check the reliable of RNA-seq, and relationship between gene expression and DMRs in the 2 kb upstream promoter region, randomly 12 common genes (EVM0016189, EVM0011007, EVM0002470, EVM0023450, EVM0021563, EVM0018643, EVM0016113, EVM0034957, EVM0014544, EVM0040816, EVM0002892, EVM0030754) of DEGs and DMRs were selected to do real-time PCR. Verification of the consistency

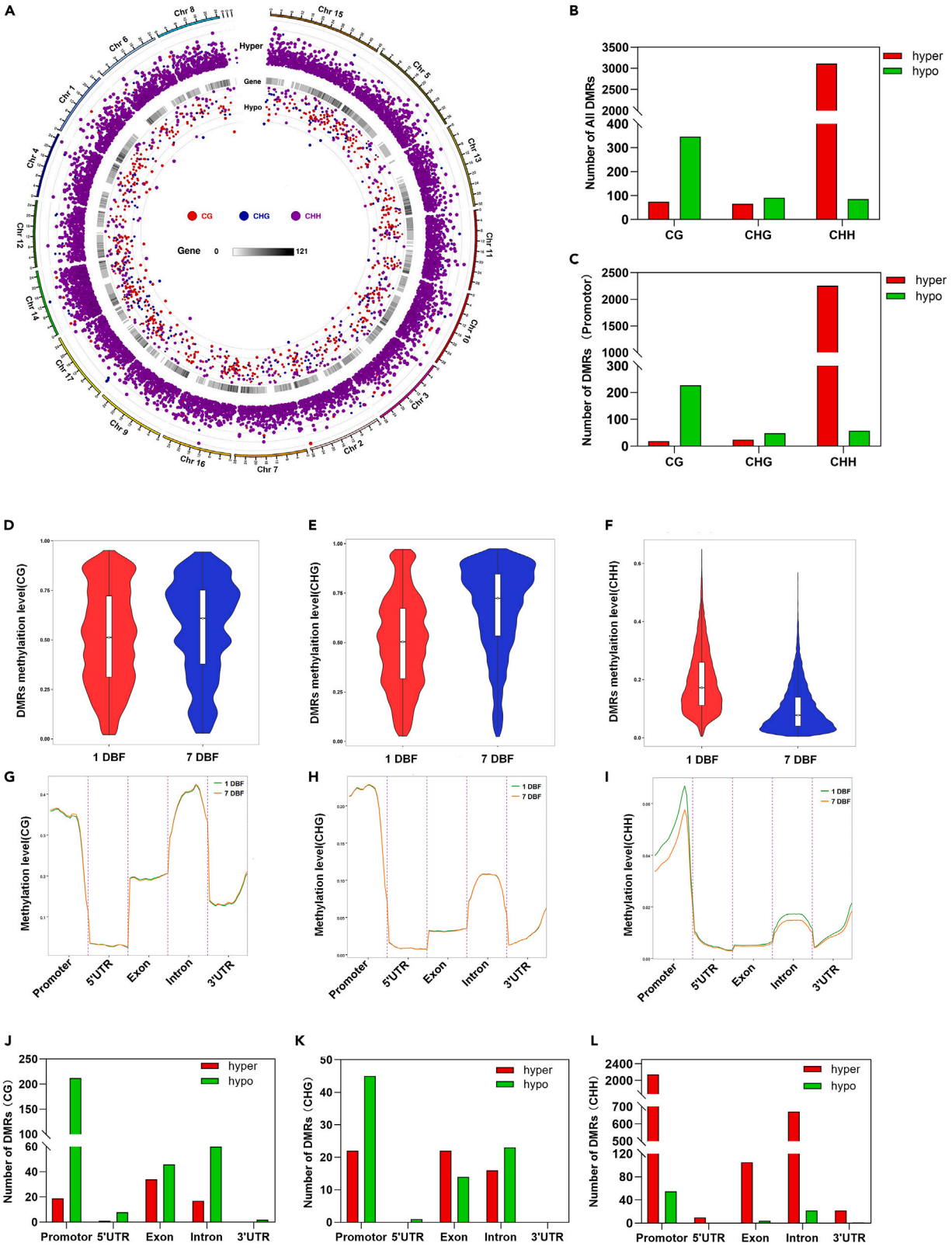
A
Chr 8
Chr 15
Chr 6
Hyper
Chr 5
Chr 1
Gene
Chr 13
Chr 4
Hypo
CG
CHG
CHH
Chr 12
Gene 0 121
Chr 11
Chr 14
Chr 10
Chr 17
Chr 3
Chr 9
Chr 2
Chr 16
Chr 7
B
Number of All DMRs
hyper
hypo
CG
CHG
CHH
C
Number of DMRs (Promotor)
hyper
hypo
CG
CHG
CHH
D
DMRs methylaition level(CG)
1 DBF
7 DBF
E
DMRs methylaition level(CHG)
1 DBF
7 DBF
F
DMRs methylaition level(CHH)
1 DBF
7 DBF
G
Methylation level(CG)
1 DBF
7 DBF
Promoter
5'UTR
Exon
Intron
3'UTR
H
Methylation level(CHG)
1 DBF
7 DBF
Promoter
5'UTR
Exon
Intron
3'UTR
I
Methylation level(CHH)
1 DBF
7 DBF
Promoter
5'UTR
Exon
Intron
3'UTR
J
Number of DMRs (CG)
hyper
hypo
Promotor
5'UTR
Exon
Intron
3'UTR
K
Number of DMRs (CHG)
hyper
hypo
Promotor
5'UTR
Exon
Intron
3'UTR
L
Number of DMRs (CHH)
hyper
hypo
Promotor
5'UTR
Exon
Intron
3'UTR

Figure 3. Statistics of different methylation forms of differentially methylated region (DMRs)
(A) Differences in genome-wide methylation levels in 1 DBF vs. 7 DBF styles.
(B and C) Numbers of different types DMRs in 1 DBF vs. 7 DBF styles.
(D–F) Average methylation levels of different types DMRs in 1 DBF and 7 DBF styles genome.
(G–I) Distribution of DNA methylation level in different transcription elements of the genome.
(J–L) Numbers of different types DMRs in gene element regions.

of qRT-PCR, RNA-seq and WGBS of that 12 genes were showed in Figures 5A–5I. The gene expression trends obtained by qRT-PCR and RNA-seq were consistent, and the R^2 value was about 0.86 (Figure 5M), further demonstrating our RNA-seq results' reliability.

The results of transcriptome and real-time PCR showed that the vast majority of the increased methylation in gene promoter regions would lead to the downregulation of transcription (Figures 5A–5I), and vice versa. R^2 value of consistency and linear regression analysis between qRT-PCR and WGBS was about 0.86 (Figure 5N).

Interestingly, significant changes in methylation levels of some genes did not cause significant changes in transcription levels (Figure 5O). The association analysis of DNA methylation and transcriptome showed that there were 237 genes with downregulated DEGs and upregulated DMRs in the 2 kb upstream promoter region, 42 genes with upregulated DEGs and downregulated DMRs in the 2 kb upstream promoter region, in style growth process (Figure 5O). Combining the enrichment results with gene annotation information, DMRs and DEGs regulated style growth were related to multiple metabolic pathways, including plant hormone signal transduction, plant-pathogen interaction and Starch and sucrose metabolism (Table S6).

DEGs and DMRs involved in the biosynthesis, metabolism and signaling transduction of plant hormones during style growth

Hormone signal pathway is the pathway with the high concentration of DEGs and DMRs, and several pathways related to hormone synthesis have been found in the secondary metabolic pathway, such as: tryptophan metabolism, alpha-linolenic acid metabolism, and carotenoid biosynsis. The relevant differential genes are shown in the Figure 6. The figures were drawn by PowerPoint 2013 based on the KEGG result.

In the pathway of tryptophan degradation (Figure 6A), indole-3-pyruvate monooxygenase (YUC), aldehyde dehydrogenase (ALDH) and amidase are the key enzymes of IAA synthesis. Upregulation of expression level of three encoding ALDH and two encoding YUC is the main reason for IAA accumulation. DMRs of three ALDH genes and three YUC genes were also observed. The decreased Amidase was not related to IAA content. Among the DEGs involved in the IAA signal transduction (Figure 6H), most genes of transport-inhibitor-resistant 1 (TIR1) protein, IAA protein, auxin response factors (ARF) protein and Gretchen Hagen3 (GH3) protein were downregulated, and only some small auxin-up RNAs (SAUR) were upregulated. The DMRs of those genes were upregulated, which corresponded to the downregulation of these DEGs.

The gene encoding xanthoxin dehydrogenase (XanDH) is upregulated (Figure 6G), consistent with increased ABA content. At the same time 9-cis-epoxy carotenoid dioxygenase (NCED) may not be directly related to ABA concentration. In addition, the expression of cytochrome P450 (CYP707A) involved in ABA degradation was downregulated during style growth, which may also be one of the reasons for ABA accumulation. Consistent with the downregulation of these DEGs, the DMRs of these genes were upregulated, indicating DNA methylation participates in regulating these gene expressions. ABA receptors (PYL), serine/threonine-protein kinase (SnRK2), and ABA-responsive element binding factor (ABF) are upregulated in the transmission pathway, while protein phosphatase 2C (PP2C) have different expression patterns (Figure 6N). In contrast, DMRs involved in ABA signal transduction were all upregulated.

In the pathway of BR synthesis, the differentially expressed genes encoding cytochrome P450 enzyme: CYP90B, CYP90C1, CYP92A6, and CYP85A1/2, are all upregulated (Figure 6C), which is consistent with the increase of BR content. The differential genes encoding brassinosteroid signaling kinase (BSK), brassinosteroid insensitive2 (BIN2), BRI1-interacting protein (BKI1), and brassinazole-resistant 1/2 (BZR1/2) participate in BR signal transduction (Figure 6J). At the same time, few DMRs were involved in BR synthesis and signal transduction.

The lipoxygenase (LOX), allene oxide synthase (AOS), allene oxide cyclase (AOC), 12-oxophydioate reductase (12-OPAR), OPC8:0-CoA ligase (OPCL) involved in JA synthesis showed a downward trend (Figure 6E), which may be the reason for the decrease of JA content. Consistent with these results, the DMRs of 12-OPAR and OPCL were upregulating. Despite the ACYL-CoA oxidase (ACX), ketoacyl-CoA thiolase (KAT) showed an upward trend. In the JA signal transmission pathway, seven encoded JASMONATE ZIM DOMAIN-CONTAINING proteins (JAZ) and one MYC2 protein were downregulated, and two JASMONIC ACID AMIDO SYNTHETASE (JAR) proteins were upregulated (Figure 6L). The DMRs of JAZ were also upregulated. These results indicated DMRs also involve in JA synthesis and signal transduction.

In addition, there are some differential genes involved in the synthesis of ETH, GA, and CTK hormones (Figures 6B, 6D, and 6F), such as S-adenosylmethionine synthesis (SAMS), 1-aminocyclopane-1-carboxylate synthesis (ACS), 1-aminocyclopane-1-carboxylate oxidation (ACO), gibberellin 20 oxidation (GA20OX), gibberellin 3 oxidation (GA3OX), gibberellin 2 oxidation (GA2OX), adenylate isopentenyl transferase (IPT), cytochrome P450 enzyme (CYP2OX 735A). In the transmission route (Figures 6I, 6K, and 6M), cytokinin receptor (CRE1), histidine-containing phosphotransfer protein (AHP), two-component response regulators (ARR), gibberellin receptor (GID1), Della, transcription factor (TF) PIF3-like, EIN3-binding F box protein (EBF1/2), ethylene-responsive transcription factor (ERF1/2) also showed differential expression. The DMRs trends of ACS and ERF1/2 were consistent with that of DEGs, which indicated DMRs also involve in ETH synthesis and signal transduction.

DEGs and DMRs involved in carbohydrate biosynthesis and metabolism during style growth

Invertase (INV), hexokinase (HXK), fructokinase (FRK), and glucose-6-phosphate isomerase (PGI) are critical enzymes that catalyze the synthesis of fructose and glucose. In this study, two genes encoding INV, one gene encoding HXK, two genes encoding FRK, and two genes

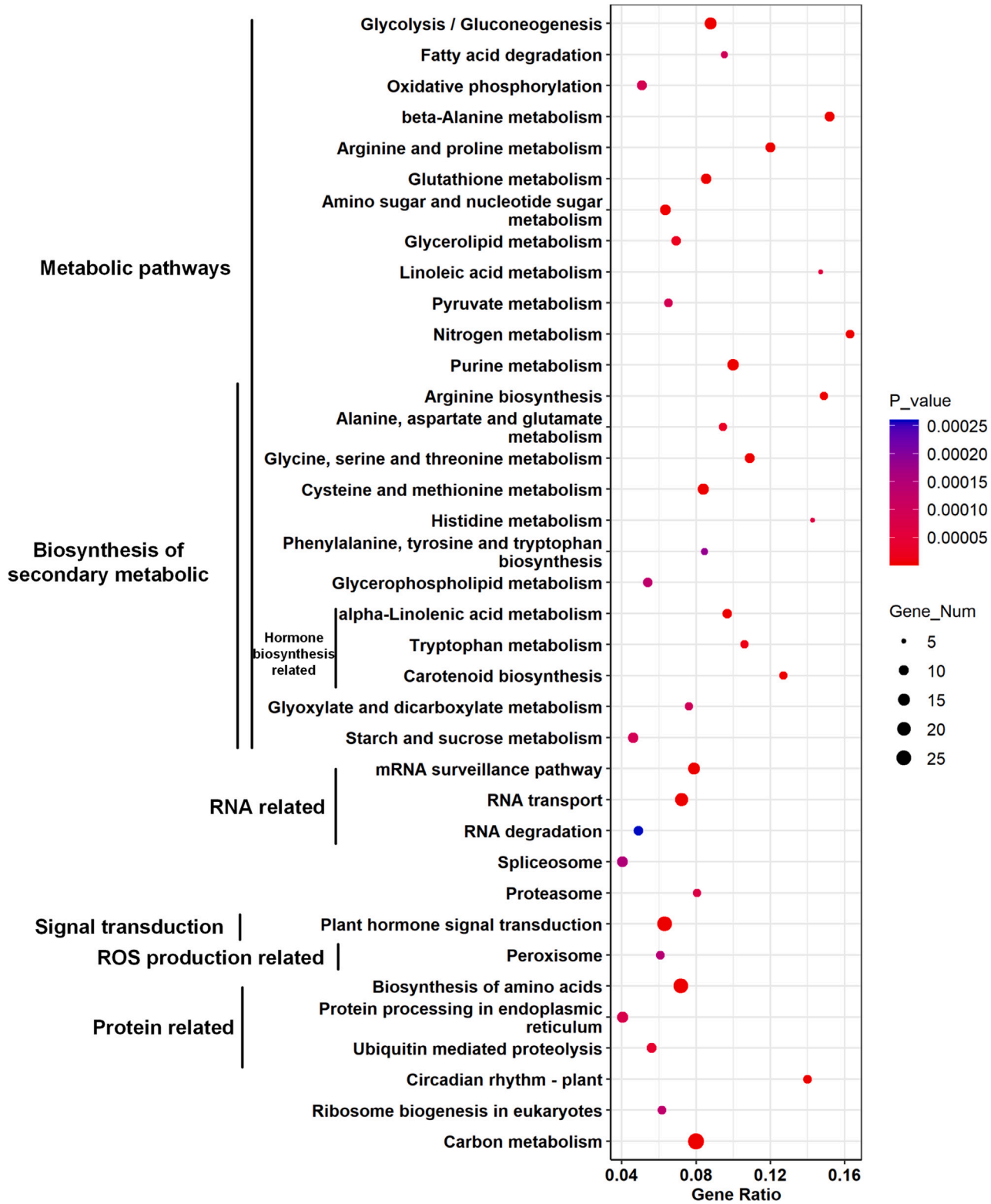

Figure 4. Scatterplot of the DMRs of promotor region identified significantly enriched KEGG pathways

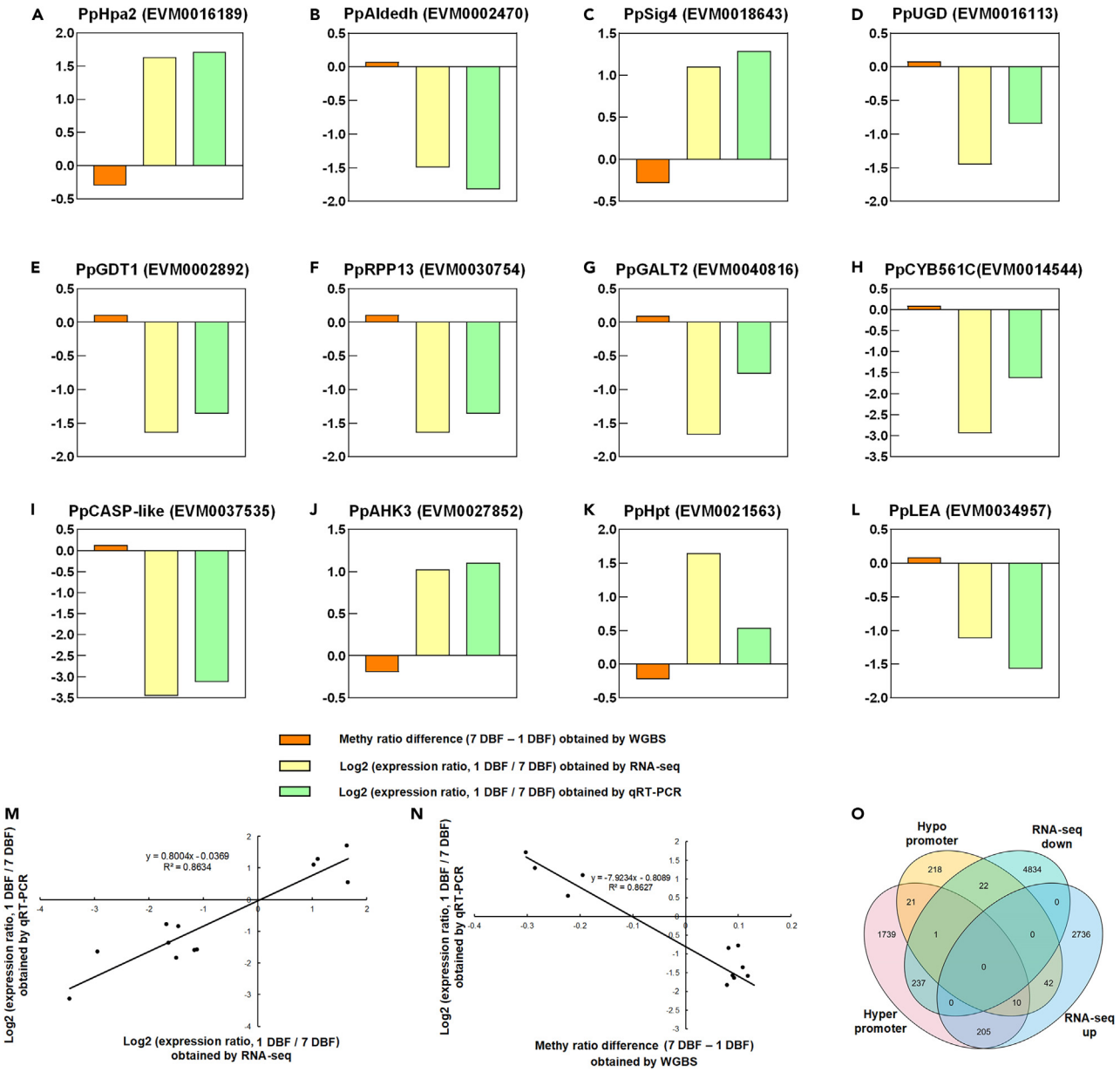

Figure 5. Consistency and linear regression analysis of the transcriptome and the whole-genome bisulfite sequencing (WGBS) data by qRT-PCR

(A–L) Verification of the consistency of RNA-seq data and WGBS data by qRT-PCR.

(M) Linear regression analysis of the transcriptome data by qRT-PCR.

(N) Linear regression analysis WGBS data by qRT-PCR.

(O) Venn diagram of common genes between DEGs and DMRs in promotor region. Venn diagram were drawn by TBtools.[20]

encoding PGI were identified with significantly increased expression from 7 DFB to 1 DFB (Figure 7). The expression levels encoding ADP-glucose pyrophosphorylase (AGPase), starch synthase (SS), and granule-bound starch synthase (GBSS), which were involved in starch synthesis, were differentially expressed. Meanwhile, the DEGs associated with starch degradation, including two α-amylase (AMY) encoding genes and six β-amylase (BAM) encoding genes, were downregulated during style growth. While, the enzymes involved in the interconversions between starch and sucrose, such as phosphoglucomutase (PGM), sucrose phosphate synthase (SPS), and sucrose phosphate phosphatase (SPP), were identified with coding genes significantly upregulated during style growth. DMRs involved in carbohydrate biosynthesis and metabolism were all up-regulated, including genes encoding HXK, UDP-glucose pyrophosphorylase (UGPase), PGM, SS, Maltase, amylomaltase, BAM. This result is mostly inconsistent with the expression of related genes.

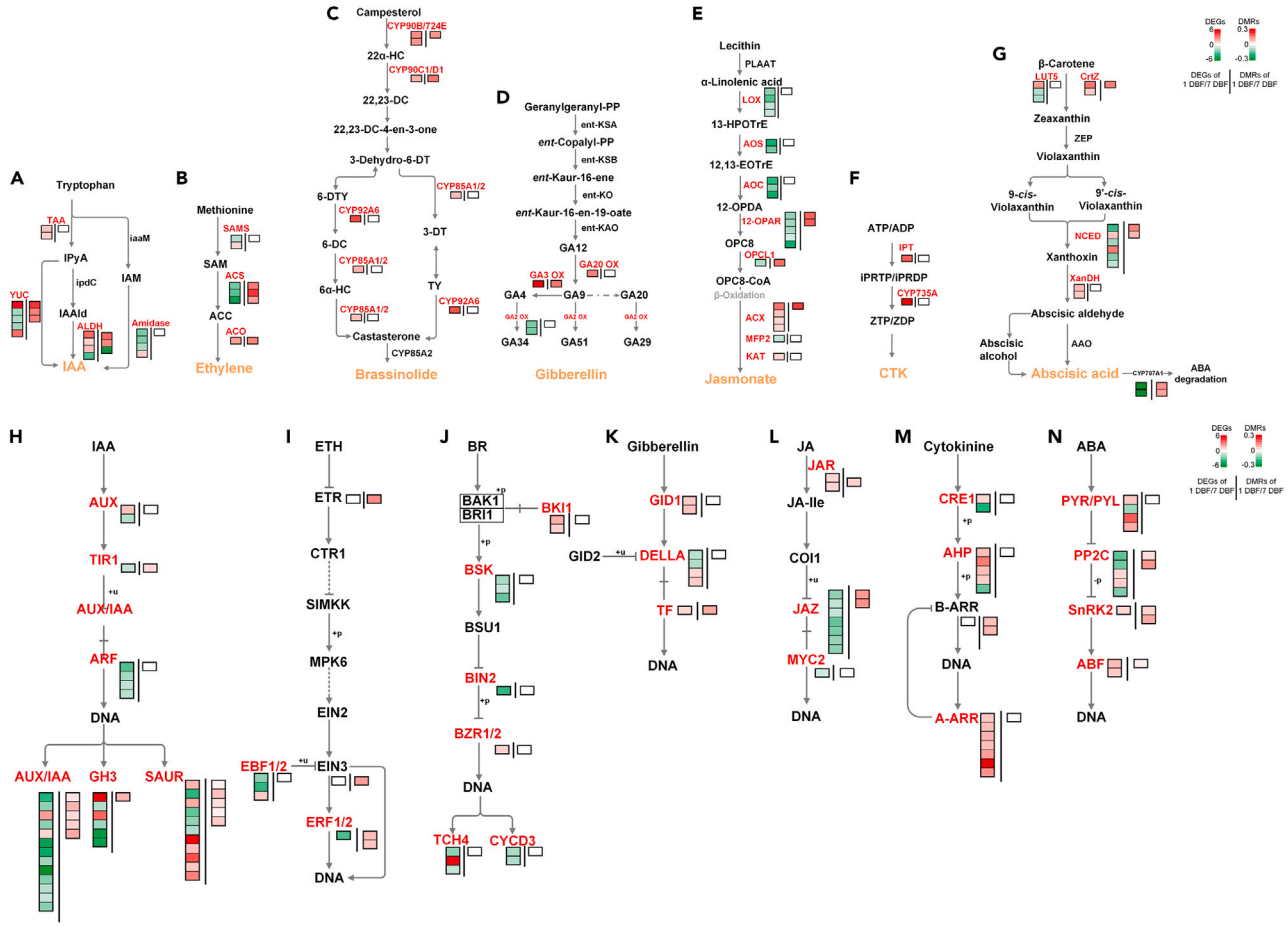

Figure 6. Regulatory model of DEGs and DMRs involved in pathways related to plant hormone biosynthesis, degradation, signaling and response

IAA (A, H), ETH (B, I), BR (C, J), GA (D, K), and JA (E, L), CTK (F, M), ABA (G, N). Each small box represents a DEG or a DMR, the red ones indicate up-regulated DEGs/DMRs, and the green ones indicate downregulated DEGs/DMRs. The white ones indicate no DEGs/DMRs were identified.

DEGs and DMRs involved TFs during style growth

Given the crucial role of TFs in regulating genes expression, we analyzed the DEGs of TF gene families that during style growth. A total of 378 TFs of DEGs most identified from bHLHs (71 genes, 18.3%), NACs (55 genes, 14.2%), WRKYs (50 genes, 12.9%), ERFs (45 genes, 11.6%), MYBs (31 genes, 8%), and bZIPs (30 genes, 7.8%) (Figure 8). Among them, most of the DEGs exhibited a downward trend during the style growth. These results indicated that expression of related genes is reduced through TFs after the style matures. Consistent with these results, most of the DMRs of TFs were upregulated, which indicated the DNA methylation involved in the TFs expression regulation.

DISCUSSION

From 7 DBF to 1 DBF, the style is in a rapid growth process. We found DEGs were involved in secondary metabolism biology, including cutin, suberin, and wax biosynthesis, phenylpropanoid biosynthesis (Figure 2), and most genes were downregulated (Table S3). And these substances are essential for style growth. The DEGs involved in cutin, suberin, and wax biosynthesis were also observed in the pistil development in papaya.[9] The decrease in related genes expression indicates slowdown in style growth and reduced demand for cell and cell wall synthesis.

Plant hormones play an important role in regulating plant growth and development, including pistil development.[9] During pear style growth, BR, IAA, and ABA reach their highest content at 1 DBF, and JA reaches their lowest (Figure 1), when the style is mature. During the development of *Arabidopsis* pistil, Auxin plays a vital role.[21] Auxin can regulate style growth by regulating *AtARF3*.[22] *AtARF3* functions as an auxin gradient interpreter and interacts with indehiscent, replumless, brevipedicellus, and Seuss to direct morphogenesis.[21,23] In pear style growth, we found four downregulated *PpARFs* DEGs (Figure 6), the results indicated that the rapid growth of the style is accompanied by high expression of these *PpARFs* genes, which decreases after the style matures. However, at 1 DBF, the content of IAA in the pear style is increased, which is inconsistent with *PpARFs* genes expression. The reasons behind this result require further research.

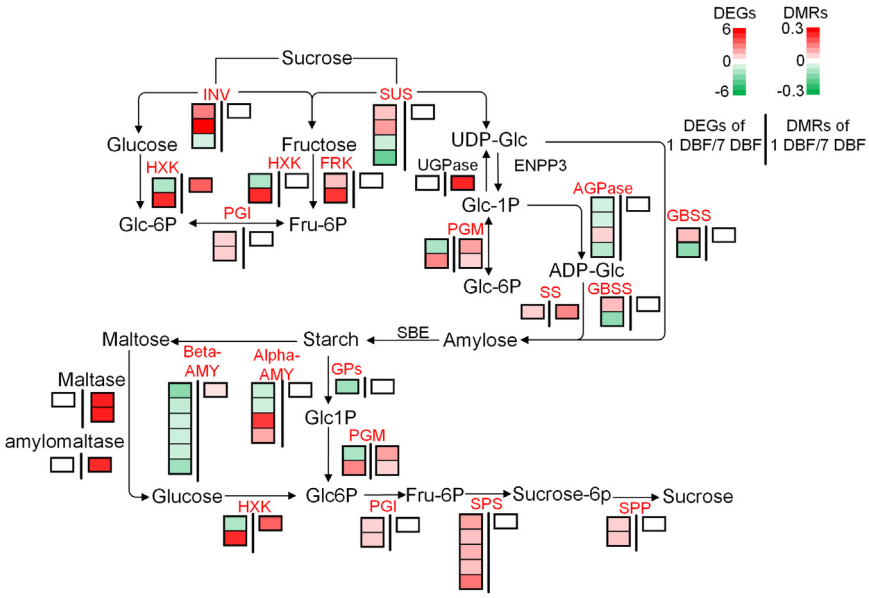

Figure 7. Regulatory model of DEGs and DMRs involved in starch and sucrose metabolism pathways in pear styles growth regulation

Each small box represents a DEG or a DMR, the red ones indicate upregulated DEGs/DMRs, and the green ones indicate downregulated DEGs/DMRs. The white ones indicate no DEGs/DMRs were identified.

BR are regulators of cell expansion. The inactivation of BRs has a clear potential role in regulating pistil length.[8] We found the BR increased during style growth. And DEGs involved in BR synthesis were all upregulated (Figure 6). These results indicated that cell expansion of style is likely to occur from 3 DBF to 1 DBF in pear. Furthermore, 12 DEGs are involved in BR signal transduction, indicating BR can regulate relative gene expression to mediated style growth. JA plays an important role in diverse processes ranging from root growth, floral development and maturation, and fruit ripening to plant defenses against insects and pathogens.[5,24,25] We found that JA had a greater content in the style at 7 DBF, indicating an inhibitory impact in controlling the growth of the pear style. Similar results were showed that JAs found to control the synchrony and velocity of floral organ growth in tobacco.[5] In our results, the JA content subsequently decreased and remained stable. The expression of DEGs encoding LOX, AOS, AOC, 12-OPAR, OPCL1, and MFP2 related to JA synthesis was reduced, and the DEGs of JAZ and MYC2 were all downregulated in JA signal transduction.

ABA is a very important plant hormone. However, the function of ABA in floral development has received less attention. Interestingly, we found ABA content rapidly increased at 1 DBF (Figure 1). DEGs involved in ABA synthesis including two *PpCrtZ* genes and two *PpXanDH* genes, were upregulated, and two *PpCYP707A1* genes responsible for ABA degradation were downregulated (Figure 6). These gene expression trends are consistent with changes in ABA content. The stigma of pear style is wet with a sugar-containing secretion, is easily infected by bacteria. Improving stigma resistance and avoiding bacterial invasion is an important task for styles. ABA plays an important role in improving plant resistance. 12 DEGs were found in ABA signal transduction, including 4 *PpPYR/PpPYL* genes, 5 *PpPP2C* genes, 1 *PpSnRK2* gene, and 2 *PpABF* genes. Furthermore, 91 DEGs were involved in the plant-pathogen interaction KEGG pathway (Figure 2D). These gene expression changes may be aimed at improving plant resistance.

The secretion of pear stigma provides the necessary material conditions for pollen germination. Polysaccharide is one of them.[13,14] We found that fructose significantly increased on 1 DBF. In addition, sucrose decreased on 3 DBF and rose to its original level at 1 DBF. Glucose gradually decreases from 7 DBF to 3 DBF and increases again on 1 DBF. However, there was no significant difference between the 1 DBF and 3 DBF or 5 DBF (Figure 1). These results indicate that the increased sugar content in the stigma of the style prepares for pollination. Consistent with this result, many DEGs identified in the 1 DBF styles sample compared to the 7 DBF styles sample are enriched in carbohydrate biosynthesis and metabolism pathway (Figure 7). Although *Brassica* has a dry stigma, DEGs are also enriched in carbohydrate biosynthesis and metabolism pathway during the maturation process of *Brassica* stigma.[26] These results indicated carbon metabolism is an important physiological process during style maturation, whether it is with dry or wet stigma. In addition to serving as a nutrient during plant growth, sugars can act as a signaling substance in coordination with hormones to regulate plant growth and development.[27] Therefore, the changes in the sugars contents of the style and stigma may also be related to the regulation of the growth of the style and stigma.

TFs play important roles in regulating gene expression. 378 TFs in DEGs were identified (Figure 8; Table S3). The most common transcription factors among these DEGs were bHLHs (71 genes, 18.3%), NACs (55 genes, 14.2%), WRKYs (50 genes, 12.9%), ERFs (45 genes, 11.6%), MYBs (31 genes, 8%), and bZIPs (30 genes, 7.8%). Similarly, bHLHs, NACs, MYBs, and bZIPs were reported to participate in the pistil development in papaya.[9] And bHLHs, NACs, MYBs, and bZIPs also involved in pistil abortion in Japanese apricot.[19] In addition, we found that a

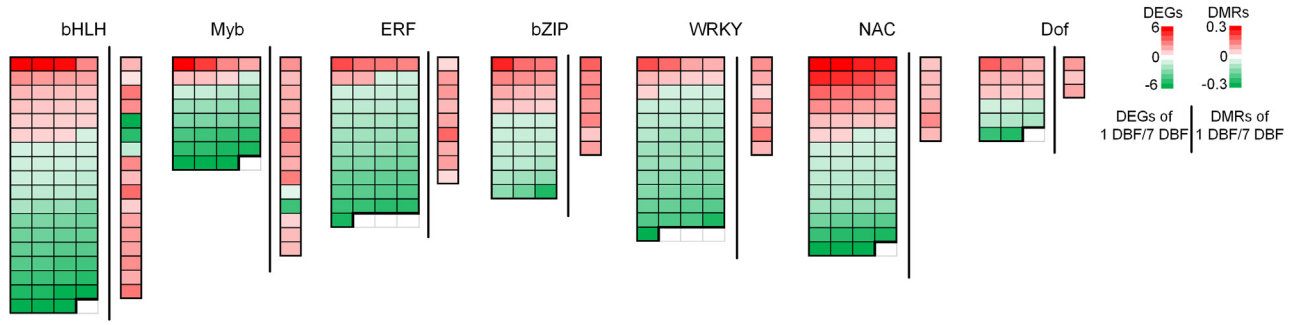

Figure 8. Clustering analysis of the DEGs and DMRs related to transcription factors

Each small box represents a DEG or a DMR, the red ones indicate up-regulated DEGs/DMRs, and the green ones indicate down-regulated DEGs/DMRs. The white ones indicate no DEGs/DMRs were identified.

large number of ERF genes are involved in the regulation of pear style growth. The ERF family is related to floral organ development.[28] However, this is the first report on the correlation between ERF and style development of fruit plants.

DNA methylation is a common epigenetic modification closely related to gene expression regulation, transposon silencing, and heterochromatin formation.[29] DNA methylation-mediated suppression prevents the transcription factors from binding to their target sequence and possibly by altering chromatin structure.[29] In current study, we identified 3771 DMRs in styles samples (Figure 3), which suggests that DNA methylation involved in pear style growth regulation. In the methylation type of DMRs, CHH accounts for 84.75%. CHH methylation is the main form of *de novo* DNA methylation in plants.[30] These indicate that *de novo* methylation is involved in the regulation of pear style growth. *De novo* DNA methylation may regulate the expression of multiple key genes involved in reproductive organ development in rice.[11] Based on the important regulatory effect of the promoter region on DNA methylation, we analyzed the DMRs in the 2 kb upstream promoter region. These DMRs are involved in cutin, suberin, and wax biosynthesis, phenylpropanoid biosynthesis, plant hormones biosynthesis, metabolism and signaling transduction, carbohydrate biosynthesis and metabolism, and TFs expression regulation (Figure 4). In current study, integrated physiological analyses, transcriptome, and DNA methylation revealed that some genes related to style growth are regulated through methylation, including many TFs genes for gene expression regulation (Figure 8). Interestingly, most of the DMRs of TFs were up-regulated. Recently, increased DNA methylation in the promoters of most genes during pear flesh development were also observed.[31] This may be because some of the necessary substances for style growth are no longer needed for synthesis after the style matures. By inhibiting TFs expression through DNA methylation, the goal of stopping style growth is achieved. This is the first discovery that DNA methylation regulates fruit tree-style growth.

In conclusion, during the development of the style and stigma, by regulating hormone synthesis related genes such as BR and IAA, as well as high expression of sucrose synthesis related genes, the style and stigma BR and IAA are increased, promoting style and stigma maturation, and preparing polysaccharides for pollination. After the maturation of the style and stigma, *de novo* methylation inhibits the expression of a large number of transcription factors further inhibiting the growth and synthesis of related substances in the style and stigma cells after the style and stigma matures.

Limitations of the study

In this study, we reveal the regulatory mechanism of pear flower stigma-style complex growth and development through physiological analyses, transcriptome, and DNA methylation, but do not involve the role of specific genes in it. Follow-up studies can determine the characteristics and regulatory mechanisms of specific genes in the process of pear flower stigma-style complex development from the pathways we have screened, which will help us better understand the regulation mechanism of pear flower style development.

STAR★METHODS

Detailed methods are provided in the online version of this paper and include the following:

- KEY RESOURCES TABLE
- RESOURCE AVAILABILITY
  - Lead contact
  - Materials availability
  - Data and code availability
- EXPERIMENTAL MODEL AND STUDY PARTICIPANT DETAILS
  - Pear styles collection
- METHOD DETAILS
  - Style length measurement

- Measurements of hormones, sugars and starch
- RNA extraction, transcriptome sequencing and samples correlation coefficient analysis
- Whole-genome bisulfite sequencing (WGBS)
- Real-time PCR and linear regression analysis

- QUANTIFICATION AND STATISTICAL ANALYSIS

SUPPLEMENTAL INFORMATION

Supplemental information can be found online at https://doi.org/10.1016/j.isci.2024.110372.

ACKNOWLEDGMENTS

This work was supported by the Key Research and Development Program (Modern Agriculture) of Jiangsu Province (BE2022381), the National Key Research and Development Program of China (2018YFD1000107), the National Natural Science Foundation of China (32370340), Key Research and Development Program (Modern Agriculture) of Baoying County (BY202215), and Jiangsu Agricultural Science and Technology Innovation Fund (CX(23)3065).

AUTHOR CONTRIBUTIONS

X.H. and C.W. designed the experiments and wrote the manuscript; X.H., L.Z., X.K., J.Z., and X.L. performed the experiments and analyzed the data.

DECLARATION OF INTERESTS

The authors declare that there is no conflict to interest.

Received: February 16, 2024
Revised: April 16, 2024
Accepted: June 21, 2024
Published: June 24, 2024

REFERENCES

1. Renner, S.S. (2014). The relative and absolute frequencies of angiosperm sexual systems: Dioecy, monoecy, gynodioecy, and an updated online database. Am. J. Bot. *101*, 1588–1596. https://doi.org/10.3732/ajb.1400196.
2. Li, W.W., Huang, X.R., Zou, J., Wu, J.J., Jiao, H.W., Peng, X.B., and Sun, M.X. (2020). Three stigma and style stylists pattern the fine architectures of apical gynoecium and are critical for male gametophyte-pistil interaction. Curr. Biol. *30*, 4780–4788.e5. https://doi.org/10.1016/j.cub.2020.09.006.
3. Gotelli, M.M., Lattar, E.C., Zini, L.M., and Galati, B.G. (2017). Style morphology and pollen tube pathway. Plant Reprod. *30*, 155–170. https://doi.org/10.1007/s00497-017-0312-3.
4. Ding, B.Q., Li, J.J., Gurung, V., Lin, Q.S., Sun, X.M., and Yuan, Y.W. (2021). The leaf polarity factors SGS3 and YABBYs regulate style elongation through auxin signaling in *Mimulus lewisii*. New Phytol. *232*, 2191–2206. https://doi.org/10.1111/nph.17702.
5. Stitz, M., Hartl, M., Baldwin, I.T., and Gaquerel, E. (2014). Jasmonoyl-l-isoleucine coordinates metabolic networks required for anthesis and floral attractant emission in wild tobacco (*Nicotiana attenuata*). Plant Cell *26*, 3964–3983. https://doi.org/10.1105/tpc.114.128165.
6. Li, J.C., Schuman, M.C., Halitschke, R., Li, X., Guo, H., Grabe, V., Hammer, A., and Baldwin, I.T. (2018). The decoration of specialized metabolites influences stylar development. Elife *7*, e38611. https://doi.org/10.7554/eLife.38611.
7. Dang, X.J., Zhang, Y.Q., Li, Y.L., Chen, S.Q., Liu, E.B., Fang, B.J., Liu, Q.M., She, D., Dong, Z.Y., Fan, Z.L., et al. (2022). SYL3-k increases style length and yield of F-1 seeds via enhancement of endogenous GA_4 content in *Oryza sativa* L. pistils. Theor. Appl. Genet. *135*, 321–336. https://doi.org/10.1007/s00122-021-03968-y.
8. Huu, C.N., Kappel, C., Keller, B., Sicard, A., Takebayashi, Y., Breuninger, H., Nowak, M.D., Baurle, I., Himmelbach, A., Burkart, M., et al. (2016). Presence versus absence of CYP734A50 underlies the style-length dimorphism in primroses. Elife *5*, e17956. https://doi.org/10.7554/eLife.17956.
9. Liao, Z., Dong, F., Liu, J., Xu, L., Marshall-Colon, A., and Ming, R. (2022). Gene regulation network analyses of pistil development in papaya. BMC Genom. *23*, 8. https://doi.org/10.1186/s12864-021-08197-7.
10. Tu, Z., Xia, H., Yang, L., Zhai, X., Shen, Y., and Li, H. (2022). The roles of microRNA-Long Non-coding RNA-mRNA networks in the regulation of leaf and flower development in *Liriodendron chinense*. Front. Plant Sci. *13*, 816875. https://doi.org/10.3389/fpls.2022.816875.
11. Wang, L., Zheng, K., Zeng, L., Xu, D., Zhu, T., Yin, Y., Zhan, H., Wu, Y., and Yang, D.-L. (2022). Reinforcement of CHH methylation through RNA-directed DNA methylation ensures sexual reproduction in rice. Plant Physiol. *188*, 1189–1209. https://doi.org/10.1093/plphys/kiab531.
12. Edlund, A.F., Swanson, R., and Preuss, D. (2004). Pollen and stigma structure and function: The role of diversity in pollination. Plant Cell *16*, S84–S97. https://doi.org/10.1105/tpc.015800.
13. de Graaf, B.H.J., Derksen, J.W.M., and Mariani, C. (2001). Pollen and pistil in the progamic phase. Sex. Plant Reprod. *14*, 41–55. https://doi.org/10.1007/s004970100091.
14. Rejón, J.D., Delalande, F., Schaeffer-Reiss, C., Carapito, C., Zienkiewicz, K., Alché, J.D., Rodríguez-García, M.I., Van Dorsselaer, A., and Castro, A.J. (2013). Proteomics profiling reveals novel proteins and functions of the plant stigma exudate. J. Exp. Bot. *64*, 5695–5705. https://doi.org/10.1093/jxb/ert345.
15. Nakanishi, T.M., Saeki, N., Maeno, M., Ozaki, T., Kawai, Y., and Ichii, T. (1991). Ultrastructural study on the stylar transmitting tissue in Japanese pear. Sex. Plant Reprod. *4*, 95–103. https://doi.org/10.1007/BF00196494.
16. Zhang, S.L., and Hiratsuka, S. (1999). Variations in S-protein levels in styles of Japanese pears and the expression of self-incompatibility. J. Jpn. Soc. Hortic. Sci. *68*, 911–918.
17. Łotocka, B., Wysokińska, E., Pitera, E., and Szpadzik, E. (2023). Ultrastructure of receptive stigma and transmitting tissue at anthesis in two pear species. Acta Agrobot. *76*, 169344. https://doi.org/10.5586/aa/169344.
18. Zhao, T., Cheng, L., Chen, C.-L., Wu, Y.-X., Wang, H., Zhang, J.-Q., Zhu, Y.-F., and Wang, Y.-X. (2022). Microstructural observation on pistil abortion of 'Li Guang' apricot and transcriptome reveal the mechanism of endogenous hormones involved in pistil abortion. Sci. Hortic. *293*, 110749. https://doi.org/10.1016/j.scienta.2021.110749.

19. Shi, T., Iqbal, S., Ayaz, A., Bai, Y., Pan, Z., Ni, X., Hayat, F., Saqib Bilal, M., Khuram Razzaq, M., and Gao, Z. (2020). Analyzing differentially expressed genes and pathways associated with pistil abortion in Japanese apricot *via* RNA-seq. Genes-Basel *11*, 1079. https://doi.org/10.3390/genes11091079.
20. Chen, C.J., Chen, H., Zhang, Y., Thomas, H.R., Frank, M.H., He, Y.H., and Xia, R. (2020). TBtools: an integrative toolkit developed for interactive analyses of big biological data. Mol. Plant *13*, 1194–1202. https://doi.org/10.1016/j.molp.2020.06.009.
21. Nemhauser, J.L., Feldman, L.J., and Zambryski, P.C. (2000). Auxin and ETTIN in *Arabidopsis* gynoecium morphogenesis. Development *127*, 3877–3888.
22. Simonini, S., Deb, J., Moubayidin, L., Stephenson, P., Valluru, M., Freire-Rios, A., Sorefan, K., Weijers, D., Friml, J., and Ostergaard, L. (2016). A noncanonical auxin-sensing mechanism is required for organ morphogenesis in Arabidopsis. Genes Dev. *30*, 2286–2296. https://doi.org/10.1101/gad.285361.116.
23. Simonini, S., Stephenson, P., and Ostergaard, L. (2018). A molecular framework controlling style morphology in *Brassicaceae*. Development *145*, dev158105. https://doi.org/10.1242/dev.158105.
24. Feys, B., Benedetti, C.E., Penfold, C.N., and Turner, J.G. (1994). *Arabidopsis* mutants selected for resistance to the phytotoxin coronatine are male sterile, insensitive to methyl jasmonate, and resistant to a bacterial pathogen. Plant Cell *6*, 751–759. https://doi.org/10.1105/tpc.6.5.751.
25. Li, L., Li, C., and Howe, G.A. (2001). Genetic analysis of wound signaling in tomato: Evidence for a dual role of jasmonic acid in defense and female fertility. Plant Physiol. *127*, 1414–1417.
26. Robinson, R., Sollapura, V., Couroux, P., Sprott, D., Ravensdale, M., Routly, E., Xing, T., and Robert, L.S. (2021). The *Brassica* mature pollen and stigma proteomes: preparing to meet. Plant J. *107*, 1546–1568. https://doi.org/10.1111/tpj.15219.
27. Ljung, K., Nemhauser, J.L., and Perata, P. (2015). New mechanistic links between sugar and hormone signalling networks. Curr. Opin. Plant Biol. *25*, 130–137. https://doi.org/10.1016/j.pbi.2015.05.022.
28. Kunst, L., Klenz, J.E., Martinez-Zapater, J., and Haughn, G.W. (1989). AP2 gene determines the identity of perianth organs in flowers of *Arabidopsis thaliana*. Plant Cell *1*, 1195–1208. https://doi.org/10.1105/tpc.1.12.1195.
29. Saze, H., Tsugane, K., Kanno, T., and Nishimura, T. (2012). DNA methylation in plants: relationship to small RNAs and histone modifications, and functions in transposon inactivation. Plant Cell Physiol. *53*, 766–784. https://doi.org/10.1093/pcp/pcs008.
30. Zhang, H.M., Lang, Z.B., and Zhu, J.K. (2018). Dynamics and function of DNA methylation in plants. Nat. Rev. Mol. Cell Biol. *19*, 489–506. https://doi.org/10.1038/s41580-018-0016-z.
31. Gu, C., Pei, M.S., Guo, Z.H., Wu, L., Qi, K.J., Wang, X.P., Liu, H., Liu, Z.C., Lang, Z.B., and Zhang, S.L. (2024). Multi-omics provide insights into the regulation of DNA methylation in pear fruit metabolism. Genome Biol. *25*, 70. https://doi.org/10.1186/S13059-024-03200-2.
32. Pan, X., Welti, R., and Wang, X. (2010). Quantitative analysis of major plant hormones in crude plant extracts by high-performance liquid chromatography–mass spectrometry. Nat. Protoc. *5*, 986–992. https://doi.org/10.1038/nprot.2010.37.
33. Liu, X., Huang, X., Kong, X.X., Zhang, J., Wang, J.Z., Yang, M.L., and Wang, C.L. (2020). Sucrose synthase is involved in the carbohydrate metabolism-based regulation of seed dormancy release in Pyrus calleryana Decne. J. Horticult. Sci. Biotechnol. *95*, 590–599. https://doi.org/10.1080/14620316.2020.1740612.
34. Zhang, J., Qian, J.-Y., Bian, Y.-H., Liu, X., and Wang, C.-L. (2022). Transcriptome and metabolite conjoint analysis reveals the seed dormancy release process in callery pear. Int. J. Mol. Sci. *23*, 2186. https://doi.org/10.3390/ijms23042186.
35. Brown, J., Pirrung, M., and McCue, L.A. (2017). FQC Dashboard: integrates FastQC results into a web-based, interactive, and extensible FASTQ quality control tool. Bioinformatics *33*, 3137–3139. https://doi.org/10.1093/bioinformatics/btx373.
36. Bolger, A.M., Lohse, M., and Usadel, B. (2014). Trimmomatic: a flexible trimmer for Illumina sequence data. Bioinformatics *30*, 2114–2120. https://doi.org/10.1093/bioinformatics/btu170.
37. Kim, D., Paggi, J.M., Park, C., Bennett, C., and Salzberg, S.L. (2019). Graph-based genome alignment and genotyping with HISAT2 and HISAT-genotype. Nat. Biotechnol. *37*, 907–915. https://doi.org/10.1038/s41587-019-0201-4.
38. Liao, Y., Smyth, G.K., and Shi, W. (2014). featureCounts: an efficient general purpose program for assigning sequence reads to genomic features. Bioinformatics *30*, 923–930. https://doi.org/10.1093/bioinformatics/btt656.
39. Wesolowski, S., Birtwistle, M., and Rempala, G. (2013). A comparison of methods for RNA-seq differential expression analysis and a new empirical bayes approach. Biosensors *3*, 238–258. https://doi.org/10.3390/bios3030238.
40. Feng, H., Conneely, K.N., and Wu, H. (2014). A Bayesian hierarchical model to detect differentially methylated loci from single nucleotide resolution sequencing data. Nucleic Acids Res. *42*, e69. https://doi.org/10.1093/nar/gku154.
41. Wu, H., Xu, T.L., Feng, H., Chen, L., Li, B., Yao, B., Qin, Z.H., Jin, P., and Conneely, K.N. (2015). Detection of differentially methylated regions from whole-genome bisulfite sequencing data without replicates. Nucleic Acids Res. *43*, e141. https://doi.org/10.1093/nar/gkv715.
42. Park, Y., and Wu, H. (2016). Differential methylation analysis for BS-seq data under general experimental design. Bioinformatics *32*, 1446–1453. https://doi.org/10.1093/bioinformatics/btw026.
43. Livak, K.J., and Schmittgen, T.D. (2001). Analysis of relative gene expression data using real-time quantitative PCR and the 2(-Delta Delta C(T)) method. Methods *25*, 402–408. https://doi.org/10.1006/meth.2001.1262.
44. Wang, G., Guo, Z., Wang, X., Guan, S.L., Gao, H., Qi, K., Gu, C., and Zhang, S. (2022). Identification and testing of reference genes for qRT-PCR analysis during pear fruit development. Biologia *77*, 2763–2777. https://doi.org/10.1007/s11756-022-01087-7.
45. Chen, J.Q., Li, X.Y., Wang, D.Q., Li, L.T., Zhou, H.S., Liu, Z., Wu, J., Wang, P., Jiang, X.T., Fabrice, M.R., et al. (2015). Identification and testing of reference genes for gene expression analysis in pollen of Pyrus bretschneideri. Sci. Hortic. *190*, 43–56. https://doi.org/10.1016/j.scienta.2015.04.010.

STAR★METHODS

KEY RESOURCES TABLE

REAGENT or RESOURCE	SOURCE	IDENTIFIER
Chemicals, peptides, and recombinant proteins		
Methyl jasmonate	Sigma-Aldrich	Cat# W341002
Brassinolide	Macklin	Cat# B803282
Abscisic acid	Sigma-Aldrich	Cat# A1049
3-Indoleacetic acid	Sigma-Aldrich	Cat# 45533
Methanol	Sigma-Aldrich	Cat# 34860
Formic acid	Sigma-Aldrich	Cat# 1.59013
Dinitrosalicylic acid	Solarbio	Cat# D7800
Sucrose	Macklin	Cat# S818048
Glucose	Macklin	Cat#D823520
Fructose	Macklin	Cat#F832295
Oligo (dT) magnetic beads	NEB	Cat#S1419S
Critical commercial assays		
TRIzol kit	Thermo Fisher	Cat#A33250
EZ DNA Methylation-Gold™ Kit	Zymo Research	Cat#D5005
SuperScript™ III First-Strand Synthesis System	Invitrogen	Cat#18080051
SsoAdvanced™ SYBR® Green Supermix	Bio-Rad	Cat#1725275
Deposited data		
RNA-seq and WGBS	NCBI	PRJNA986301
Software and algorithms		
HISAT2 2.0.5	https://daehwankimlab.github.io/hisat2/	HISAT2
DESeq2 1.20.0	https://github.com/thelovelab/DESeq2	DESeq2
KOBAS 3.0	http://genome.cbi.pku.edu.cn/download.html	KOBAS
Fastp 0.20.0	https://github.com/OpenGene/fastp/blob/master/README.md	Fastp
Bismark 0.16.3	http://www.bioinformatics.bbsrc.ac.uk/projects/bismark/.	Bismark
Bismark	http://bowtie-bio.sourceforge.net/bowtie2/index.shtml.	Bismark
Fastqc	http://www.bioinformatics.babraham.ac.uk/projects/fastqc/	Fastqc

RESOURCE AVAILABILITY

Lead contact

Further information and requests for resources and reagents should be directed to and will be fulfilled by the lead contact, Chun-Lei Wang (wangcl@yzu.edu.cn).

Materials availability

This study did not generate new unique reagents. All key resources are listed in the key resources table.

Data and code availability

- This paper does not report original code.
- The RNA-seq and WGBS data have been deposited at NCBI and are publicly available as of the date of publication. Accession numbers are listed in the key resources table.
- Any additional information required to reanalyze the data reported in this paper is available from the lead contact upon request.

EXPERIMENTAL MODEL AND STUDY PARTICIPANT DETAILS

Pear styles collection

Pear styles with stigma were collected from *Pyrus pyrifolia* 'Cuiguan' adult trees planted in the orchards of Yangzhou University, Jiangsu, China. Flowers were collected 7, 5, 3, 1, and 0 days before anthesis, the flowers of different trees serve as biological replicates. The collection time is from 10:00 to 11:00 AM in a good weather day. The styles were detached with stigma on ice. Collect the styles of every 50 flowers within 5 minutes, concentrate them in the same centrifuge tube, and weigh them for storage in liquid nitrogen.

METHOD DETAILS

Style length measurement

In order to measure the length of the style, styles from different periods were immediately measured with a Vernier caliper after being removed. Styles of 30 flowers from three different trees were measured per period. The data were presented as means ± standard error (SE). All data were tested by ANOVA and the means were compared using Tukey's test. $P < 0.05$ indicated statistically significant differences.

Measurements of hormones, sugars and starch

The styles with stigmas of five periods (7 DBF, 5 DBF, 3 DBF, 1 DBF, and 0 DBF) were used to determine the content of hormones, starch, and hormones. The extraction of hormones (ABA, BR, JA, and IAA) from 0.1 g style sample was followed the method described previously.[32] Styles from three different trees serve as three biological replicates. High-performance liquid chromatography–electrospray ionization–mass spectrometry (Agilent 1200 UHPLC/6460 QQQ, Santa Clara, CA, USA) was used to measure the hormone content. Chromatographic column is Agilent Eclipse plug C18 column (150 mm × 2.1 mm × 5 μm). Methanol (mobile phases A) and 0.1% (v/v) formic acid (mobile phases B) as mobile phases were followed the the program: 10% A and 90% B for 2 min, 40% A and 60% B for 13 min; 100% A for 2min, 10% A and 90% B for 8 min.

The determination methods for starch and sugar refer to the article we previously published.[33,34] The starch content from 0.1 g style sample was measured by the dinitrosalicylic acid (DNS) method. Styles from three different trees serve as three biological replicates. Soluble sugars, including sucrose, glucose, and fructose were measured from 0.1 g style sample. Styles from three different trees serve as three biological replicates.

RNA extraction, transcriptome sequencing and samples correlation coefficient analysis

The total RNAs were isolated by using TRIzol kit (Thermo Fisher, Shanghai, China), followed by manufacturer's instructions. The mRNA enriched by Oligo (dT) magnetic beads (NEB, IL, USA) was randomly interrupted and synthesized cDNA. After undergoing end repair and A-tailed addition, the cDNA around 370-420 bp was used to obtain the library. The concentration of total RNA, RIN value, 28S/18S and fragment sizes were detected by Qubit 2.0 Fluorometer and Agilent 2100 bioanalyzer. When the RNA concentration exceeds 100 ng/μl, the total amount exceeds 10 μg, and RNAs with high purity (RIN ≥ 7) were used to construct sequencing libraries. RNA-seq was run on Illumina platform (Illumina, CA, USA). The FastQC was used to evaluate the quality of raw sequencing data, including checking sequence quality, sequence length distribution, and GC content.[35] Based on the evaluation results, Trimmomatic was used to remove low-quality sequencing sequences, splice sequences, and low-quality bases.[36] High quality clean reads were compared to 'Cuiguan' genome (https://ngdc.cncb.ac.cn/gwh/Assembly/18534/show) through HISAT2.[37] FeatureCounts (1.5.0-p3) are used to calculate the FPKM (the expected number of transcriptional sequence fragments per thousand base pairs sequenced per million base pairs) to measure gene expression levels.[38,39] In this study, |log2 fold change ≥ 1| and adjusted P value < 0.05 were used as the standards to filter for the DEGs (differentially expressed genes). The Gene Ontology (GO) and Kyoto Encyclopedia of Genes and Genomes (KEGG) databases were used for enrichment analysis of DEGs.

The samples correlation coefficient (SCC) algorithm was used to calculate the correlations between experimental values obtained from three biological replicates of samples. SCC cluster analyses were performed based on the average FPKM value of all expressed genes in 6 samples. The ggplot2 package was used to draw the correlation graph.

Whole-genome bisulfite sequencing (WGBS)

Sonication (300 W, 30 min; SCIENTZ18-A, SCIENT, Ningbo, China) was used to fragment genomic DNA (200-300 bp), and bisulfite treatment of these DNA was carried out by EZ DNA Methylation-Gold™ Kit (Zymo Research, CA, US). Library construction completed by Novogen Corporation, and its quality was detected by Agilent Bioanalyzer 2100 system. Pair-end sequencing was run on the Illumina platform (Illumina, CA, USA). DSS software was used to identify the differentially methylated regions (DMRs).[40–42] DMRs were distinguished into gene body (from transcriptional start site to Transcription termination site) or promoter region (2 kb upstream from the transcriptional start site) based on the location of 'Cuigan' genome. The KEGG databases were used for enrichment analysis of DMRs.

Real-time PCR and linear regression analysis

Total RNA was isolated from the styles with stigmas of 7 DBF and 1 DBF. RNA was reverse-transcribed by the SuperScript™ III First-Strand Synthesis System (Invitrogen, Shanghai, China). Gene-specific primers were designed using the online software Primer3 (http://primer3.ut.ee/), and the quality and specificity of each primer pair were checked by melting curve analysis. The primers used are described in

Table S1. Real-time PCR was performed with the SsoAdvanced™ SYBR® Green Supermix (Bio-Rad, Shanghai, China) on a Bio-Rad® CFX 96. The amplification procedures were as follows: a pre-denaturation step of 95°C for 3 min, 30 cycles of 95°C for 5 s and 60°C for 5 s and melting curve analysis. Quantitative PCR data were analyzed following the $2^{-\Delta\Delta CT}$ method.[43] The transcript abundance of the examined genes was normalized using the average Ct value corresponding to the *actin* gene (EVM0028888), *tubulin* gene (EVM0013735), and *ubiquitin* gene (EVM0030932). The three reference genes were selected based on our transcriptome data. These three genes are also used as reference genes for other pear tissues.[44,45] In our transcriptome data, the expression of these three genes is also stable.

In order to conduct consistency and linear regression analysis of the transcriptome and the WGBS data, randomly 12 common genes (EVM0016189, EVM0037535, EVM0002470, EVM0027852, EVM0021563, EVM0018643, EVM0016113, EVM0034957, EVM0014544, EVM0040816, EVM0002892, EVM0030754) of DEGs and DMRs were selected to do real-time PCR. To conduct linear regression analysis of the transcriptome and WGBS data by real-time-PCR, The log2 (gene expression ration of 1 DBF to 7 DBF by real-time PCR) value was as the vertical axis, and the RNA-seq log2 (fold change) or methylation ration by WGBS of same gene was as the horizontal axis value, respectively. Linear equation and correlation coefficient were calculated by Excel.

QUANTIFICATION AND STATISTICAL ANALYSIS

At least three replications were performed per experimental treatment. The data were presented as means ± standard error (SE). All data were tested by ANOVA and the means were compared using Tukey's test. $P < 0.05$ indicated statistically significant differences.